

# Current Distribution of Ecosystem Functional Types in Temperate South America

José M. Paruelo,<sup>1\*</sup> Esteban G. Jobbágy,<sup>2</sup> and Osvaldo E. Sala<sup>1</sup>

<sup>1</sup>IFEVA. *Departamento de Recursos Naturales y Ambiente, Facultad de Agronomía, Universidad de Buenos Aires, Av. San Martín 4453, Buenos Aires 1417, Argentina;* and <sup>2</sup>*Departamento de Producción Animal, Facultad de Agronomía, Universidad de Buenos Aires, Av. San Martín 4453, Buenos Aires 1417, Argentina*

## ABSTRACT

We described, classified, and mapped the functional heterogeneity of temperate South America using the seasonal dynamics of the Normalized Difference Vegetation Index (NDVI) from NOAA/AVHRR satellites for a 10-year period. From the seasonal curves of NDVI, we calculated (a) the annual integral (NDVI-1), used as an estimate of the fraction of photosynthetic active radiation absorbed by the canopy and hence of primary production, (b) the relative annual range of NDVI (RREL), and (c) the date of maximum NDVI (MMAX), both of which were used to capture the seasonality of primary production. NDVI-1 decreased gradually from the northeastern part of the study region (southern Brazil and Uruguay) toward the southwest (Patagonia). High precipitation areas dominated by rangelands had higher NDVI-1 and lower RREL values than neighboring areas dominated by crops. The relative annual range of NDVI was maximum for the northern portion of the Argentine pampas (high cover of summer crops) and the subantarctic forests in southern Chile (high cover of deciduous tree

species). More than 25% of the area showed an NDVI peak in November. Around 40% of the area presented the maximum NDVI during summer. The pampas showed areas with sharp differences in the timing of the NDVI peak associated with different agricultural systems. In the southern pampas, NDVI peaked early (October–November); whereas in the northeastern pampas, NDVI peaked in late summer (February). We classified temperate South America into 19 ecosystem functional types (EFT). The methodology used to define EFTs has advantages over traditional approaches for land classification that are based on structural features. First, the NDVI traits used have a clear biological meaning. Second, remote-sensing data are available worldwide. Third, the continuous record of satellite data allows for a dynamic characterization of ecosystems and land-cover changes.

**Key words:** remote sensing; land cover; ecosystem functioning; South America; Normalized Difference Vegetation Index; NDVI.

## INTRODUCTION

Global-scale environmental problems are challenging the traditional approaches used to describe ecosystems at large scales. Traditionally, the characterization of heterogeneity at regional or continental scales relied on the structural features of ecosystems

and focused on potential rather than current vegetation. The attributes most frequently used to classify vegetation units were the abundance of plant functional types or physiognomy (Mueller-Dombois and Ellenberg 1974). Potential vegetation units were often defined on the basis of climate, but the correspondence between vegetation and climate was seldom tested empirically (Holdridge 1947; Box 1981; Prentice and others 1992; but see Stephenson 1990). Mapping potential rather than current veg-

Received 6 October 1999; accepted 2 April 2001.  
\*Corresponding author; e-mail: paruelo@ifeva.edu.ar

etation was the aim; consequently, anthropogenic ecosystems, such as crops, cultivated pastures, tree plantations, or modified rangelands, were systematically excluded.

The structural attributes of ecosystems, such as vegetation physiognomy or the composition of plant functional types change slowly in response to human disturbances. These features tend to register the effects of climate change or pollution much later than alterations in ecosystem functioning. Inertia often characterizes the response of vegetation structure to environmental changes, as reported in studies of several ecosystems at different time scales (Pennington 1986; Malanson and others 1992; Milchunas and Lauenroth 1995). Thus, a characterization of ecosystems that is based exclusively on structural attributes may not be sensitive enough to assess the impact of current environmental changes if the response of vegetation structure has a large time lag. Ecosystem functioning, the exchange of matter and energy between the biota and the environment, has in some cases a shorter response time than structure (Myneni and others 1997). Today most terrestrial ecosystems are far from their original nonaltered or potential state. Therefore, if we want to make a valid assessment of the effects of environmental change, our understanding of the current condition of these systems needs to be based on sensitive and ecologically meaningful attributes.

Remote sensing is a valuable method that can be used to describe the spatial heterogeneity of ecosystems functioning at regional and global scales. Information derived from remotely sensed data can accurately represent functional attributes of the ecosystem such as aboveground net primary production (ANPP) (Tucker and others 1985a; Prince 1991; Paruelo and others 1997). Lloyd (1990) proposed the use of phenology, derived from the seasonal course of the Normalized Difference Vegetation Index (NDVI) obtained from NOAA/AVHRR satellites, to describe ecosystem functioning. Soriano and Paruelo (1992) proposed the use of biozones, units defined from functional ecosystem traits derived from satellite imagery. Nemani and Running (1997) devised a scheme to classify land cover into six classes based on the NDVI and temperature data derived from the NOAA/AVHRR satellites. Functional analyses based on remotely sensed data allow for a top-down characterization of ecosystem heterogeneity (Wessman 1992).

Most of the attempts to describe land-cover patterns at the global scale in recent years have been based on data obtained via remote sensing (Love-

land and others 1991; Loveland and Beldward 1997; De Fries and others 1998; Loveland and others 2000). The IGBP-DIS global land-cover data set is one of the best documented of such products (Loveland and others 2000). The seasonal dynamics of spectral indexes and individual bands provided by the AVHRR sensor on board the NOAA satellites were used to define the land-cover classes. Aside from the usefulness for global studies, the IGBP-DIS land-cover database and most of the other land-cover products available on the Internet (<http://edcdaac.usgs.gov/glcc/glcc.html>) fail to represent the current distribution of both agricultural areas and vegetation types in South America. For example, the main agricultural areas of southern South America were classified as grasslands and the areas dominated by natural grasslands as croplands. The IGBP-DIS scheme also fails to describe the main differences among the semiarid and arid land-cover types of central and southern South America. These inaccuracies may be due to the fact that this global classification, like many others, used training sites located in the Northern Hemisphere to create classification rules that were applied globally.

In this paper, we characterized the functional heterogeneity of temperate ecosystems of South America. We described, classified, and mapped current vegetation using traits derived from the seasonal dynamics of the NDVI, which captures the amount and seasonality of ANPP. In addition to the regional classification, we evaluated the association between the functional ecosystem traits and climate.

Based on our functional classification of ecosystems, we developed the concept of ecosystem functional types (EFTs). These units are defined independently of vegetation structure and focus on the exchange of the energy and matter of ecosystems. EFTs are conceptually related to plant functional types (PFTs); however, EFTs are defined at a different level of organization than PFTs. EFTs group similarly functioning ecosystems independent of structure, whereas PFTs group similarly functioning species independent of phylogeny (Chapin 1993). As PFTs may be defined according to different functional dimensions (for example, relative growth rates, nitrogen fixation, tolerance or resistance to herbivory, and so on), EFTs can be defined on the basis of different aspects of matter/energy flows. Here we focus on the dynamics of primary production, one of the essential and most integrative functional attributes of ecosystems.

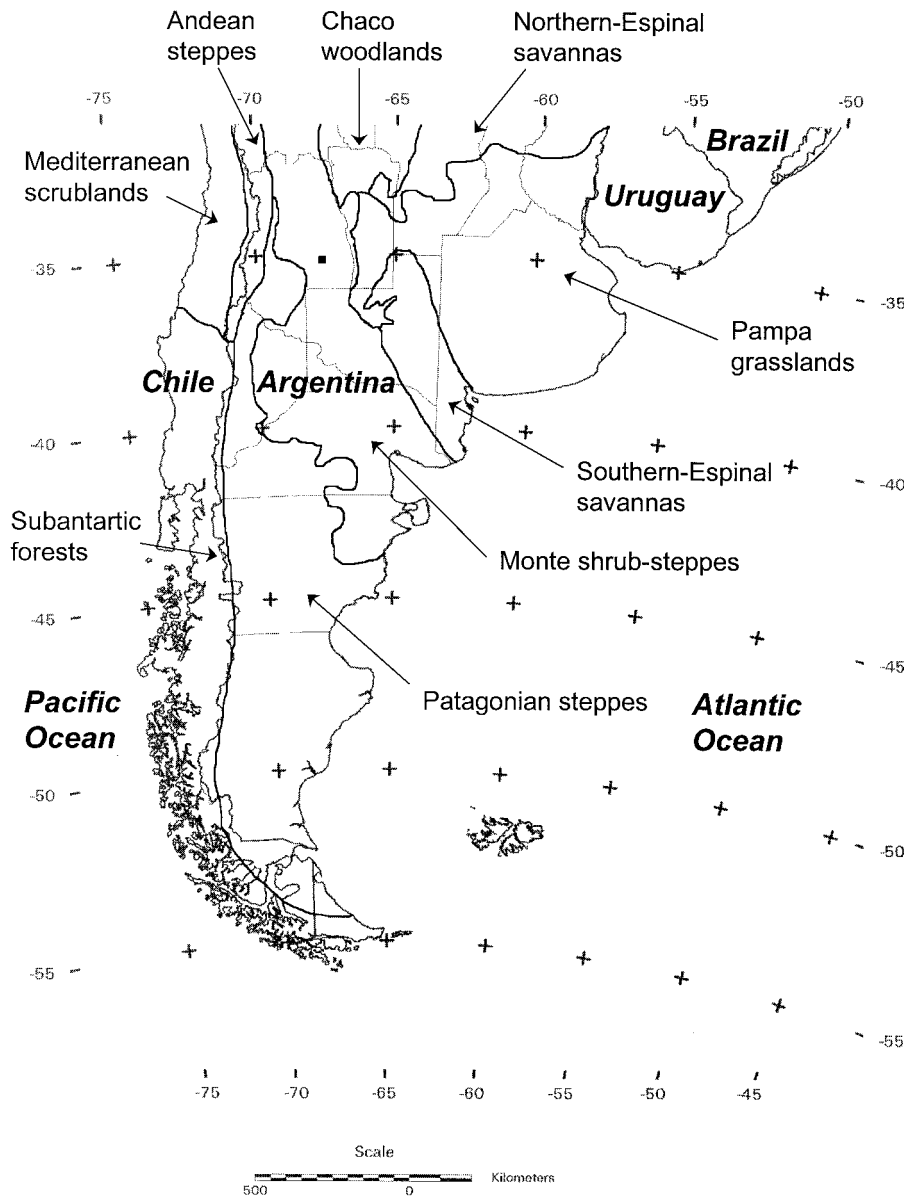


Figure 1. Phytoecographic units of temperate South America. Redrawn from Cabrera and Wilkins (1973), Paruelo and others (1991), and Soriano (1991).

**MATERIALS AND METHODS**

Our study focused on the temperate portion of South America. We set the northern boundary of the temperate zones at 30°S of latitude, which excludes most of the subtropical areas of South America (Cabrera 1976) (Figure 1). From a structural viewpoint, our work examined forests (subantarctic); woodlands (Chaco, Espinal); grasslands (la Pampa, Campos, Patagonia); scrublands (Chilean Matorral); shrub, grass and mixed steppes (Monte, Patagonia, High Andes); semideserts (Monte, Patagonia, high Andes); and annual crops and cultivated perennial pastures (Morello 1958; Cabrera

1976; Paruelo and others 1991; Soriano 1956, 1991; León and others 1998) (Figure 1).

We based our analysis on the NDVI, as determined from AVHRR/NOAA satellites. NDVI combines the spectral data of channel 1 (red, 580–680 nm) and channel 2 (near infrared, 725–1100 nm):

$$NDVI = \frac{\text{channel 2} - \text{channel 1}}{\text{channel 2} + \text{channel 1}}$$

Green vegetation shows a differential reflectance in these two bands because active photosynthetic surfaces reflect a high proportion of the incoming radiation in the infrared band and a small proportion

in the red band. We used the NOAA/NASA Pathfinder AVHRR land data set created by NASA (James and Kallury 1994). This data set comes from NOAA-7, -9, and -11 satellite imageries and was radiometrically and spatially corrected (for details see James and Kallury 1994; Rao and Chen 1995). The scenes have a spatial resolution of  $8 \times 8$  km and cover the whole globe. We used the 10-day maximum value composite for the 1982–91 period (a total of 360 images) for the portion of the images located between  $30^{\circ}\text{S}$  and  $55^{\circ}\text{S}$ . The maximum NDVI value represents the highest count registered by the satellite during a 10-day period. We built a simple program to automatically remove spurious values from the data set and to calculate a moving average with a window covering three 10-day periods. We also checked the images for temporal and seasonal trends not related to the vegetation signal by inspecting four pixels of the Atacama Desert in northern Chile (an extreme desert). Seasonal NDVI variability at the Atacama Desert was small and we assumed it was noise. The problems associated with cloud contamination, off-nadir views, and sensor degradation not removed by the original processing of the PAL database or our filtering algorithm were minimized by using a 10-year average curve of the NDVI dynamics (M. F. Garbulsy unpublished).

We extracted the essential attributes of primary production dynamics from satellite information by calculating the following three traits of the seasonal curves of NDVI: the annual integral, the relative annual range of NDVI, and the date of maximum NDVI. These traits showed a negligible correlation among each other in our data set (correlation coefficient less than 0.01) and are known to capture important features of ecosystem functioning (Nemani and Running 1997; Paruelo and others 1998). Principal component analyses of the NDVI curves showed that these traits were highly correlated with the first principal components and summarized most (more than 80%) of the spatial variability of the NDVI dynamics in temperate areas (Paruelo and others 1993; Paruelo and Lauenroth 1995).

The annual integral was calculated by summing the products of 10-year average NDVI for each period and the proportion of the year represented by that period. NDVI-1 is a good estimator of the fraction of the photosynthetic active radiation absorbed by the canopy (Sellers and others 1992) and hence of primary production (Tucker and others 1985a; Prince 1991; Paruelo and others 1997).

The relative range of NDVI corresponded to the 10-year mean difference between the annual maximum and minimum NDVI, divided by the NDVI-1.

This attribute provides a description of the intra-annual variation of the NDVI independent of NDVI-1 values. Two areas with the same NDVI-1 may have very different relative annual ranges of NDVI-1 (RREL). For example, perennial grasslands in the pampas have the same NDVI-1 as croplands but a significantly lower RREL.

The date of maximum NDVI corresponded to the month with the highest frequency (mode) of peak NDVI for the period analyzed. The relative range and the date of maximum NDVI capture essential features of the seasonality of carbon gains (Paruelo and Lauenroth 1998).

We classified all land pixels within the study area based on the three traits of the NDVI curve. We used the Iterative Self-Organizing Data Analysis (ISODATA) method to generate signatures for the humid and dry parts of the temperate regions independently (Tou and Gonzalez 1974). ISODATA is an unsupervised iterative classification technique that uses minimum distances to assign an individual pixel to a cluster. A new mean is defined in each iteration based on the location of the pixel included in the cluster in the space defined by the three NDVI attributes. We merged the signatures obtained for each subregion and established its classification using maximum likelihood as the basis for each decision (Hord 1982). We checked the statistical significance of the differences among units within the three-dimensional space defined by the NDVI attributes using canonical discriminant analysis. After merging nonsignificantly different units, we obtained 19 classes within which the pixels had similar NDVI dynamics. We defined these classes as ecosystem functional types (EFTs).

EFTs are given a code of two letters and a number (a total of three characters) based on the average value of each trait used in the definition of the classes (NDVI-1, RREL, and MMAX). The first (upper-case) letter of the code corresponds to the NDVI-1 level, ranging from *A* to *K* for high to low NDVI-1. The second (lower-case) letter shows the relative range, similarly ranging from *a* to *h* for high to low RREL. The number indicates the month of maximum NDVI (from 1 for January to 12 for December). We divided the NDVI-1 and RREL axes into intervals of 0.05 NDVI units. The definition and coding of EFTs were based only on functional attributes.

We evaluated the correspondence between the functionally defined units and potential vegetation by analyzing the distribution of the EFTs within the phytogeographical units defined on a physiognomic basis on previous studies (Morello 1958; Cabrera and Wilkins 1973; Cabrera 1976; Paruelo and oth-

ers 1991; Soriano 1956, 1991; León and others 1998). We also evaluated the correspondence between EFTs and current land-cover types based on data compiled by J. P. Guerschman and others (unpublished) at the province level using the Agricultural National Census of Argentina. For each EFT within a given phytogeographical unit, we assessed whether it occurred on natural vegetation (native forest or rangelands) or agricultural land (crops or cultivated pastures). This analysis was not intended to be an evaluation of our approach but an objective assessment of the agreement between structural and functional descriptions of ecosystems at the regional level.

To analyze the relationship between functional ecosystem traits and climate variables, we used a global climate database (Leemans and Cramer 1991) with a resolution of  $0.5^\circ$  of latitude and longitude. The database was constructed by interpolating actual climatic data from 2583 stations worldwide and includes monthly precipitation and temperature. This database has been successfully tested for South America (Paruelo and others 1995). We resampled the database from its original resolution ( $0.5 \times 0.5^\circ$ ) to the spatial resolution of the NDVI data ( $8 \times 8$  km). Because of the different resolutions of the climatic and NDVI databases, the same climatic values were assigned to more than one pixel. We performed a stepwise regression analysis on 25% of the pixels of the study area. This subset of pixels was obtained by selecting every other pixel within a row from every other row. The variables derived from the NOAA/AVHRR database were the dependent variables; mean annual temperature (MAT), mean annual precipitation (MAP), the proportion of precipitation falling during summer (December, January, and February) and winter (June, July, and August), and their logarithmic transformations were the independent variables. Statistical analyses were performed using SAS software (SAS 1988).

## RESULTS

The three attributes of the analyzed NDVI curve (NDVI-1, relative range, and month of maximum NDVI) showed clear and contrasting patterns across the temperate areas of South America (Figure 2). Average NDVI integral (NDVI-1) decreased gradually from the northeastern part of the study region (southern Brazil and Uruguay) toward the southwest (Patagonia) (Figure 2). NDVI-1 increased on the western side of the Andes (southern Chile), the area dominated by *Nothofagus* forest. Average NDVI for the 10-year period under analysis ranged be-

tween 0.456 and  $-0.032$ . Extreme values corresponded to the Uruguayan grasslands and the warm deserts of northwest Argentina, respectively. There was a bimodal distribution of the NDVI-1 values (Figure 3a). The classes with values below 0.1 and between 0.3 and 0.4 were the most frequent. Based on the relationship between NDVI-1 and ANPP presented by Paruelo and others (1997), the mean values for these classes corresponded to ANPP of  $127 \text{ kg ha}^{-1} \text{ y}^{-1}$  and  $5150 \text{ kg ha}^{-1} \text{ y}^{-1}$  respectively.

The relative range of NDVI was maximum for the northern portion of the Argentine pampas and for the subantarctic forests in southern Chile (Figure 2). The lowest values occurred across a northwest-southeast belt from the border between Chile and Argentina to the northern Patagonia coast. The relative range of NDVI showed clear discontinuities in contrast with the always gradual change in NDVI-1. For example, in the pampas, there was a sharp contrast in relative range at both sides of the Paraná River, but there were small changes in NDVI-1. The relative range of NDVI was concentrated around intermediate values and usually higher than 0.1 (Figure 3b).

The temperate ecosystems of South America differed in timing of maximum NDVI. Figure 2 shows the month with the highest frequency of maximum NDVI for the 10-year period. The peak of NDVI occurred earlier (September–October) in central Chile and the southwest portion of the pampas. Peak NDVI occurred in November in central and east Patagonia and later (December and January) in the west. The pampas showed areas with sharp differences in the timing of the NDVI peak. In the southern pampas, NDVI peaked early (October–November); whereas in the northeastern pampas, peak NDVI occurred in late summer (February). More than 25% of the area showed an NDVI peak in November. Around 40% of the area had a maximum NDVI during summer (December, January, and February) (Figure 3).

Our classification divided the temperate ecosystems of South America into 19 classes (EFTs) with different functions (Figure 4 and Table 1). Each EFT was characterized based on mean NDVI-1, relative range of NDVI, and month of maximum NDVI (Figure 5). The canonical discriminant analysis showed that the EFTs differed significantly ( $P < 0.01$ ) from each other. The square distances derived from the pooled within-class covariance matrix (Mahalanobis distance) among the centroid of every pair of EFTs was statistically significant ( $P < 0.0001$ ). The plot of the centroid of each EFT on the space of the pairwise combination of the NDVI traits showed lack of correlation among traits (Figure 5). Based on

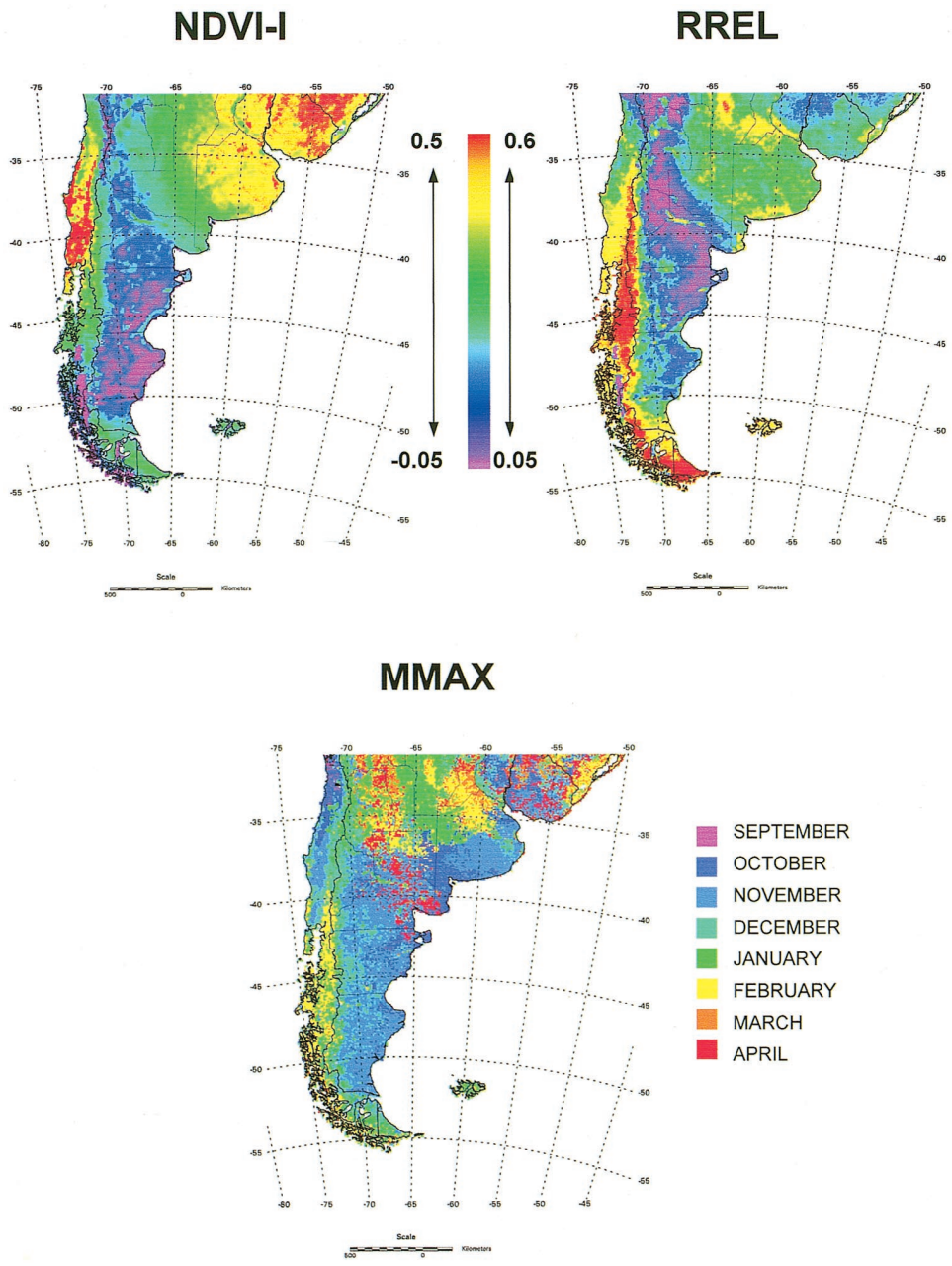


Figure 2. Maps showing the three attributes of the Normalized Difference Vegetation Index (NDVI) included in the analysis: NDVI integral (NDVI-1), the relative range of NDVI (RREL), and the month of maximum NDVI (MMAX).

the association among EFTs, phytogeographic units, and land-use patterns, we identified a structural correlate for each EFT (see Appendix).

Sixty percent of the spatial variability in NDVI-1 across temperate South America was accounted for by the following three climatic variables: mean annual precipitation (MAP), mean annual temperature (MAT), and the proportion of precipitation falling during summer (SUM) (Table 2). NDVI-1 was positively related with MAP and MAT and negatively related with SUM. Precipitation was the variable that accounted for the highest proportion of NDVI-1 variability—45% (Figure 6). When only

those points with precipitation of less than 1200 mm were considered, the proportion of the variance accounted for by precipitation increased up to 69% and the contribution of the other variables was negligible. Most of the points above 1200 mm corresponded to subantarctic forests and transitional areas where the NDVI values may be contaminated with water signals (coastal areas and islands). The interpretation of the relationship of the functional traits of these areas and climatic variables is uncertain.

Climatic variability accounted for 34% of the variability of the relative range of NDVI that de-

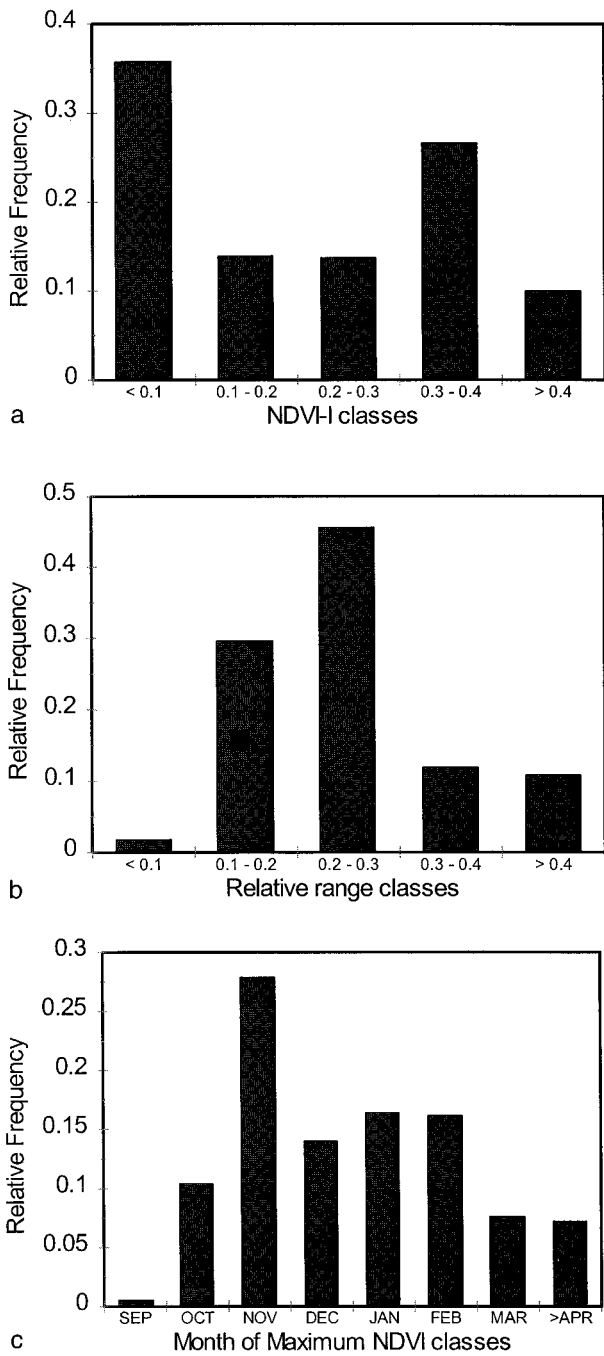


Figure 3. Frequency distributions of the three Normalized Difference Vegetation Index (NDVI) attributes: (a) NDVI integral, (b) relative range of NDVI, and (c) month of maximum NDVI.

creased with increases in MAP and MAT (Table 2). Fourteen percent of the variability in the date (month) of maximum NDVI was accounted for by climatic variables (Table 2). Maximum NDVI tended to occur later in areas where precipitation

was high and concentrated during the summer months.

More than 75% of the area of 13 EFTs was occupied by a single phytogeographic unit (Table 3). One other EFT (Jf12) included two very closely related phytogeographical units. Fe1 and Gf12 were particularly heterogeneous in terms of potential vegetation. They included areas classified as Chaco, Espinal, Pampa, and Monte. In both cases, however, the whole area had the same land use (rangeland) (Table 3).

### DISCUSSION

EFT definitions based on remote-sensing data is an objective and repeatable way to characterize the current functioning of ecosystems (Wessman and others 1999). Valentini and others (1999) pointed out the importance of defining functional units in terrestrial ecosystems based on the exchange of matter and energy in the ecosystem. This method for characterizing terrestrial ecosystems has the clear advantage of defining the exchange of trace gases and energy between the land surface and the atmosphere (Valentini and others 1999). We did not attempt to assimilate the functional classes to particular land-cover types. In fact different land covers may have similar seasonal patterns of productivity (for example, some summer crops in the pampas and the *Nothofagus* forests of the southern Andes); conversely, the same land-cover type may have different NDVI dynamics (for example, the grasslands of the Argentine and Uruguayan pampas)

Particular combinations of the three functional attributes were not represented in temperate South America. For example, there were no combinations with high NDVI-1 (first letter of the EFT code *A* and *B*) and either high (second letter of the EFT code *a* and *b*) or low relative range of NDVI (second letter of the EFT code *g* and *h*) (Figure 5). The lack of an *Aa* EFT reflects a constraint on the maximum NDVI that a particular ecosystem can reach. NDVI is related to photosynthetically active radiation (PAR) intercepted; consequently, it will reach a maximum when the canopy intercepts 100% of PAR. If the canopy is approaching 100% of IPAR (and maximum NDVI), a high RREL can be reached only if the minimum NDVI throughout the year is very low. A low NDVI in winter will reduce NDVI-1. On the other hand, an *Ah* EFT requires a high and stable NDVI through the year. Only tropical ecosystems can have these dynamics.

Climatic variability accounted for most of the spatial variability of NDVI-1, particularly for the

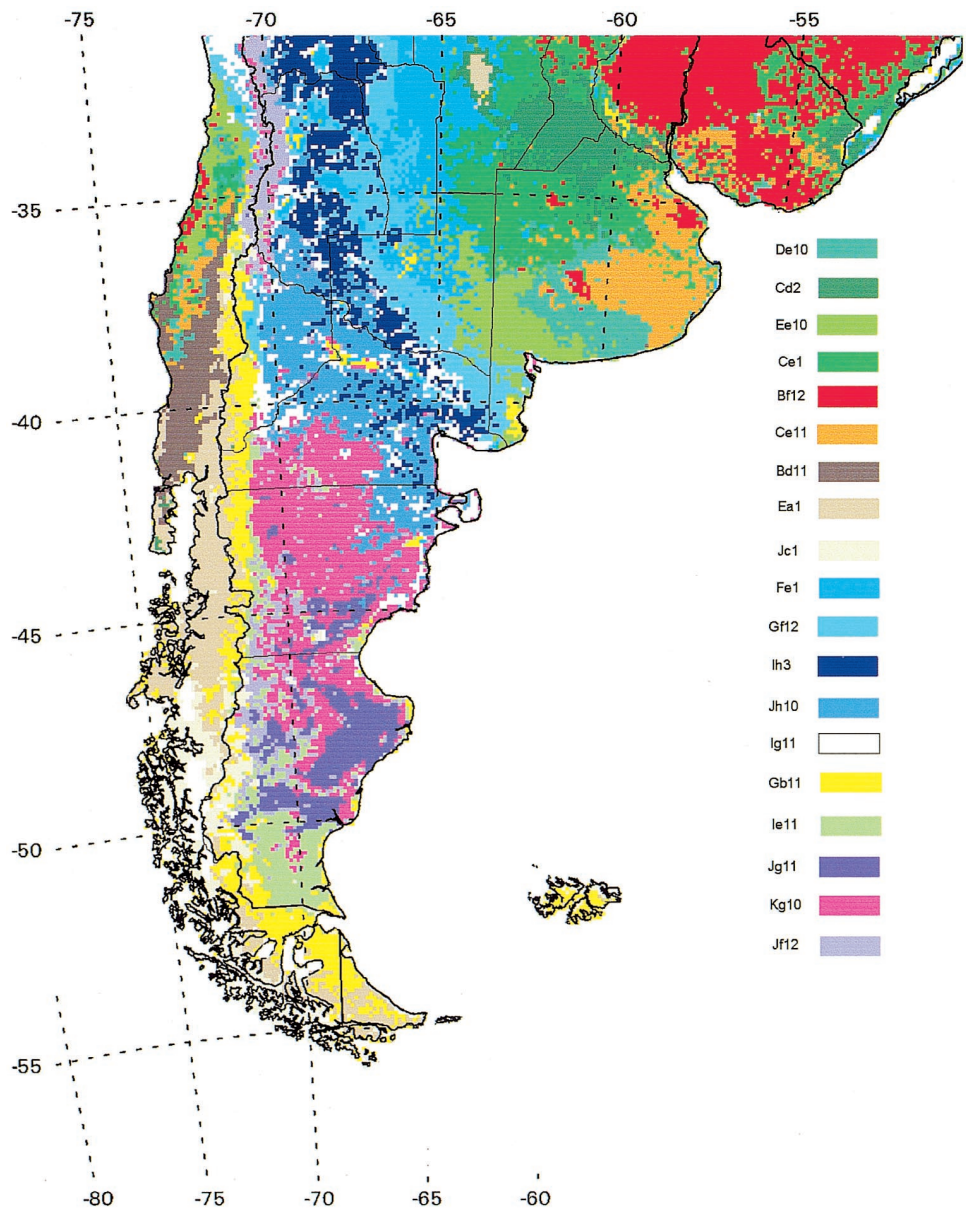


Figure 4. Map showing the ecosystem functional types (EFTs) for temperate South America.

0–1200-mm precipitation range. Previous studies found either no relationship between temperature and NDVI-1 or ANPP (Sala and others 1988; Paruelo and Lauenroth 1995, 1998) or a negative one (Epstein and others 1997). These studies were restricted to grassland or shrubland areas. However, our analysis yielded a positive relationship between MAT and NDVI-1 (Table 2). The explanation suggested for the negative relationship between temperature and precipitation in grasslands was that higher temperature results in higher potential evapotranspiration and for similar values of precipitation, less water is available for plant growth (Epstein and others 1997). This explanation is suitable only for water-limited systems. Our study region

encompasses a broad range of annual rates of precipitation, including areas where precipitation is higher than potential evapotranspiration. Temperature may have a positive effect on production in areas that are not water-limited because it extends the length of the growing season (E. G. Jobbágy and others forthcoming; Goulden and others 1996). A small proportion of the spatial variation of RREL and MMAX was associated with climatic variables. Agricultural practices may alter the seasonal dynamics of carbon gains and therefore mask the effect of climatic variables in determining ecosystem functioning.

We did not find a clear correspondence between EFT and phytogeographical provinces. A particular

**Table 1.** Temperate South American Ecosystem Functional Types (EFTs)

| Functional Code | Number | Area (km <sup>2</sup> ) | MAP (mm) | MAT (°C) |
|-----------------|--------|-------------------------|----------|----------|
| De10            | 01     | 72,192                  | 836      | 14.2     |
| Cd2             | 02     | 89,408                  | 934      | 16.4     |
| Ee10            | 03     | 89,920                  | 651      | 13.6     |
| Ce1             | 04     | 221,440                 | 988      | 16.4     |
| Bf12            | 05     | 210,752                 | 1229     | 17.5     |
| Ce11            | 06     | 95,744                  | 915      | 14.7     |
| Bd11            | 07     | 55,744                  | 1255     | 9.7      |
| Ea1             | 08     | 177,856                 | 1485     | 5.6      |
| Jc1             | 09     | 186,880                 | 1666     | 4.0      |
| Fe1             | 10     | 138,112                 | 661      | 16.0     |
| Gf12            | 11     | 146,624                 | 436      | 15.1     |
| Ih3             | 12     | 122,368                 | 279      | 13.9     |
| Jh10            | 13     | 157,568                 | 204      | 11.3     |
| Ig11            | 14     | 85,991                  | 238      | 9.7      |
| Gb11            | 15     | 180,992                 | 806      | 6.4      |
| Ie11            | 16     | 91,712                  | 357      | 3.3      |
| Jg11            | 17     | 202,560                 | 188      | 8.4      |
| Kg10            | 18     | 90,368                  | 141      | 8.5      |
| Jf12            | 19     | 98,176                  | 351      | 3.4      |

The functional code represents each EFT based on the value of the NDVI integral (first letter, uppercase), the relative range of NDVI (second letter, lowercase), and the month of maximum NDVI (1 = January, 12 = December and so on).

MAP and MAT correspond to the average mean annual precipitation and mean annual temperature of all the pixels of the region comprising a given EFT.

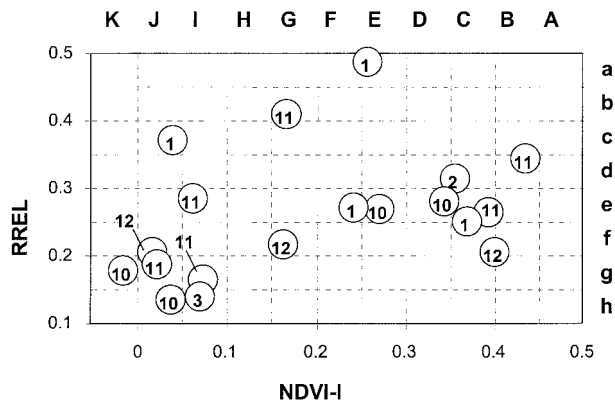


**Figure 5.** Distribution of the centroid of the ecosystem functional types (EFTs) for temperate South America in the context of NDVI integral (NDVI-I) and relative annual range of NDVI (RREL). The circled numbers represent the modal months of peak NDVI (MMAX). The letters on the axes correspond to the code used to label the EFTs in Table 1.

EFT may be present in more than one phytogeographical province, and a phytogeographical province may include more than one EFT. The differences between the structural (phytogeographical) and functional (EFT) approaches are due to the use

of different attributes to classify the ecosystem. It is possible that structurally different units have similar functioning or that structurally similar units differ in their functioning. Land-use change also accounts for some of the differences between the two approaches.

Another reason for the differences between the functional and phytogeographical classifications is that different criteria are used to set boundaries between units or to define the level of aggregation of the units. With both methods, there is a great deal of subjectivity associated with defining the limit of a unit. Many of the attributes used to define the units exhibited subtle changes across the environmental gradient (see Figure 2), and an objective definition of boundaries, either structural or functional, is difficult. It is possible that several of the EFTs defined here were part of a larger phytogeographical unit. The criteria used to define the level of aggregation varied among the phytogeographical units. By contrast, the functional classification used the same criteria of aggregation for all units (to maximize the distance of the classes in the space of the three NDVI traits).

In a functional classification of ecosystems, every pixel is classified based on its behavior. Mapping does not rely on untested models of the relationship

**Table 2.** Coefficient of Determination (R-Square), Y-Intercept, and Climatic Variables Included in the Models Relating NDVI Annual Integral (NDVI-1), Relative Annual Range of NDVI (RREL), and Month of NDVI Peak to Climate

| Attribute | R-Square | Y-Intercept | Climatic Variable | Coefficient | F    | P     |
|-----------|----------|-------------|-------------------|-------------|------|-------|
| NDVI-1    | 0.60     | −0.4307     | Log MAP           | 0.0930      | 3015 | 0.001 |
|           |          |             | MAT               | 0.0120      | 1577 | 0.001 |
|           |          |             | SUM               | −0.2904     | 408  | 0.001 |
| RREL      | 0.34     | 0.2951      | MAP               | 0.000067    | 1219 | 0.001 |
|           |          |             | MAT               | −0.006849   | 951  | 0.001 |
| MMAX      | 0.14     | 4.7137      | SUM               | 4.944       | 507  | 0.001 |
|           |          |             | MAP               | 0.000615    | 249  | 0.001 |

MAP, mean annual precipitation; MAT, mean annual temperature; SUM, summer precipitation  
 For each independent variable, the value of the coefficient and the partial F are indicated.  
 For all three models. n = 4236.

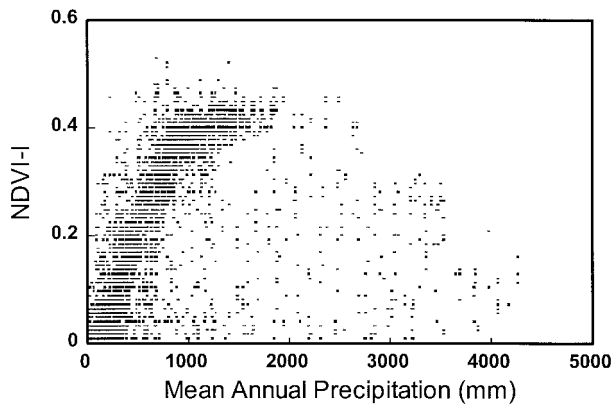


**Figure 6.** Relationship between mean annual precipitation ( $\text{mm y}^{-1}$ ) and NDVI-1 for temperate South America.

between structural attributes and environmental features (climate, soils, landscape units) to interpolate point data over an entire region. At regional scales, the relationship between environmental features and structural ecosystem attributes has not been formally tested. The use of remote sensing-based EFTs avoids the use of a rule to interpolate point or local observations up to the region. This solves an important “scaling-up” problem in regional analysis.

The use of maps showing potential vegetation imposes serious limitations on the assessment of ecosystem functioning at the global scale. All over the planet, there have been enormous changes in land use and land cover that have drastically altered many ecosystems. Forests, grasslands, savannas, and deserts have all been altered by human activity. Over the last 3 centuries, the area covered by forests

has decreased by 1.2 billion ha, or 19%, and grasslands have decreased by 560 million ha, or 8% (Richards 1993). Increases in the extent of croplands and urban areas account for most of these changes to forests and grasslands. The rate of land-use change is still accelerating in some parts of the world. Agricultural expansion, for example, was greater during the 30-year period from 1950 to 1980 than the entire 150 years between 1700 and 1850 (Richards 1993).

Our analysis suggests some general trends in the change of ecosystem functioning following the conversion of natural vegetation to agriculture. Table 4 shows some of the most dramatic changes by providing land-use data for counties that belong to the same phytogeographic unit. Villaguay ( $31^{\circ}30'S$ ,  $59^{\circ}W$ ), is a county located in the heart of the pampas, that is comprised almost entirely of natural grassland. The dominant EFT is Bf12. Caseros ( $33^{\circ}12'S$ ,  $61^{\circ}36'W$ ) corresponds to the same phytogeographical unit, but most of the area is devoted to summer crops. On a functional basis, Caseros had a lower NDVI-1 and a higher relative range, and the NDVI peaked later there than in Villaguay (EFT Cd2). A similar pattern was found for Tercero Arriba ( $33^{\circ}12'S$ ,  $64^{\circ}W$ ) and San Javier ( $32^{\circ}S$ ,  $65^{\circ}W$ ), two counties located in the Northern Espinal. Tercero Arriba, which is dominated by summer crops included EFTs with a higher interannual variability than San Javier, which is dominated by rangelands. Because the Northern Espinal has a higher proportion of precipitation in summer than the pampas, the NDVI of the natural vegetation peaked in summer. Patagones county ( $40^{\circ}S$ ,  $63^{\circ}W$ ) has 19% agricultural land (85% of which is dryland winter crops) in its eastern half (INDEC 1988). The same

**Table 3.** Correspondence of Ecosystem Functional Types (EFTs) with Potential Vegetation and Current Land Use in Temperate South America

| Number | Functional Code | Phytogeographic Unit       | %   | Current Land Use                                  |
|--------|-----------------|----------------------------|-----|---|
| 01     | De10            | Pampa grasslands           | 82  | Winter crops                                      |
|        |                 | Chilean scrublands         | 9   | Crops/Pastures/Rangeland                          |
| 02     | Cd2             | Pampa grasslands           | 82  | Summer crops                                      |
|        |                 | Northern Espinal woodlands | 13  | Summer crops                                      |
| 03     | Ee10            | Pampa grasslands           | 41  | Winter crops/Pastures                             |
|        |                 | Southern Espinal woodlands | 35  | Winter crops/Pastures                             |
|        |                 | Chilean scrublands         | 20  | Crops/Pastures/Range                              |
| 04     | Ce1             | Pampa grasslands           | 77  | Summer crops/Pasture                              |
|        |                 | Northern Espinal woodlands | 17  | Summer crops/Pasture                              |
| 05     | Bf12            | Pampa grasslands           | 78  | Rangelands (nonflooded)                           |
|        |                 | Northern Espinal woodlands | 20  | Rangelands (nonflooded)                           |
| 06     | Ce11            | Pampa grasslands           | 92  | Rangelands (flooded)                              |
| 07     | Bd11            | Subantarctic forests       | 92  | Native and planted forests                        |
| 08     | Ea1             | Subantarctic forests       | 95  | Native forests                                    |
| 09     | Jc1             | Subantarctic forests       | 96  | Native forests                                    |
| 10     | Fe1             | Chaco woodlands            | 35  | Rangelands  |
|        |                 | Northern Espinal woodlands | 23  | Rangelands  |
|        |                 | Pampa grasslands           | 19  | Rangelands  |
|        |                 | Monte shrub steppes        | 14  | Rangelands  |
|        |                 | Chaco woodlands            | 14  | Rangelands  |
| 11     | Gf12            | Chaco woodlands            | 21  | Rangelands  |
|        |                 | Southern Espinal woodlands | 14  | Rangelands  |
|        |                 | Pampa grasslands           | 9   | Rangelands  |
|        |                 | Monte shrub steppes        | 87  | Rangelands  |
| 12     | Ih3             | Chaco woodlands            | 5   | Rangelands  |
|        |                 | Monte shrub steppes        | 86  | Rangelands  |
| 13     | Jh10            | Patagonia steppes          | 12  | Rangelands  |
|        |                 | Monte shrub steppes        | 50  | Rangelands  |
| 14     | Ig11            | Patagonia steppes          | 23  | Rangelands  |
|        |                 | Chilean scrublands         | 12  | Rangelands  |
|        |                 | Patagonia steppes          | 69  | Rangelands  |
| 15     | Gb11            | Patagonia steppes          | 69  | Rangelands  |
|        |                 | Subantarctic forests       | 25  | Rangelands (grassland areas within native forest) |
| 16     | Ie11            | Patagonia steppes          | 97  | Rangelands  |
| 17     | Jg11            | Patagonia steppes          | 91  | Rangelands  |
| 18     | Kg10            | Patagonia steppes          | 100 | Rangelands  |
| 19     | Jf12            | Patagonia steppes          | 73  | Rangelands  |
|        |                 | High Andes steppes         | 23  | Rangelands  |

*Phytogeographic units in which EFTs occur correspond to potential vegetation. Percentage indicates the proportion of all the area covered by an EFT in temperate South America that occurs within a given phytogeographic unit. All of the phytogeographic units that cover at least 90% of the whole area of an EFT are shown. Dominant current land use for each EFT within a given phytogeographical unit is indicated.*

percentage—19%—of the county is occupied by Gb11 in the same portion. The rest of the county, as well as most of the arid belt of Southern Espinal, is currently occupied by rangelands and corresponds to Gf12. It is likely that Gb11 is replacing Gf12 in this area (Figure 7). Irrigated crops within Northern and Southern Monte and Patagonia seem to converge into the same EFT: Gb11. In the foothills of

the Andes in Mendoza (33°S, 68°30'W) and in the Rio Negro (39°S, 67°30'W) and Chubut (43°18'S, 65°30'W) valleys, EFT Gb11 coincides with areas devoted to irrigated crops (INDEC 1988). Adjacent areas are occupied by rangelands corresponding to EFTs Ih3, Jh10, and Kg10 for each one of these areas, respectively (Figure 7). These preliminary data suggest that both dryland and irrigated agri-

**Table 4.** Correspondence between Land Use and Ecosystem Functional Type (EFT) Distribution in the Pampas and Northern Espinal

| County           | Sum | Win | Pas | Range | Dominant EFT         |
|------------------|-----|-----|-----|-------|----------------------|
| Pampas           |     |     |     |       |                      |
| Villaguay        | 4   | 5   | 5   | 86    | Bf12 (100%)          |
| Caseros          | 50  | 24  | 15  | 12    | Cd2 (100%)           |
| Northern Espinal |     |     |     |       |                      |
| Tercero Arriba   | 63  | 12  | 7   | 18    | Ea1 (53%), Cd2 (38%) |
| San Javier       | 3   | 1   | 6   | 90    | Fe1 (74%), Ce1 (26%) |

*Sum, summer crops; Win, winter crops; Pas, cultivated pastures*  
*The proportion of dominant EFTs is shown for counties with contrasting land use within the same phytogeographic unit.*  
*All cases reflect dryland agriculture.*

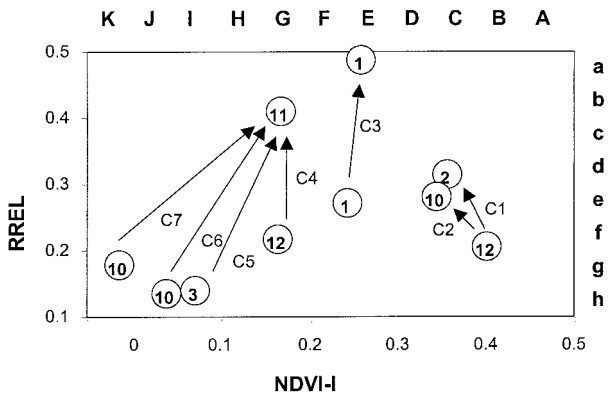


**Figure 7.** Hypothetical trajectories of functional changes in ecosystems after conversion to agriculture. The centroid of ecosystem functional types (EFTs) is shown in the context of NDVI integral (NDVI-I) and relative annual range of NDVI (RREL). Circled numbers indicate the modal months of peak NDVI. C1 and C2 represent conversion from nonflooded rangeland (Bf12) to dryland summer (Cd2) and winter (De10) crops in the pampas. C3 represents a shift from xerophytic woodlands (Fe1) to dryland summer crops (Ea1) in the Northern Espinal. C4 shows the conversion from scrubland (Gf12) to dryland winter crops (Gb11) in the Southern Espinal. C5, C6, and C7 represent the introduction of irrigated crops (mostly perennial) (Gb11) in Patagonia (Kg10) and Monte (Jh10, Ih3). All of the conversions to agriculture involve an increase in RREL.

culture modify the seasonality of carbon gains (J. Paruelo and others unpublished). The NDVI integral seems to decrease slightly under dryland agriculture in the pampas and to have no change in the Northern and Southern Espinal. Irrigated agriculture, by contrast, would increase NDVI-I. Dryland agriculture in the pampas caused dramatic changes in the month of NDVI peak, delaying or anticipating

it by approximately 2 months in the case of summer and winter crops, respectively (trajectories C1 and C2, in Figure 7).

The methodology used to define ecosystem functional types has additional advantages over traditional approaches based on structural features. First, the NDVI traits have a clear biological meaning. They capture the essential characteristics of carbon dynamics (Tucker and others 1985b; Malingreau 1986; Lloyd 1990, Nemani and Running 1997; Wessman and others 1999). Second, remote-sensing data are available worldwide, making it possible to characterize, monitor, and compare ecosystems globally using the same data set. Third, the continuous record of satellite data allows for a dynamic characterization of ecosystems as well as the monitoring of land-cover changes.

**ACKNOWLEDGMENTS**

This work was funded by the Inter-American Institute for Global Change Research (ISP3 077 and PESCA 010), the Universidad de Buenos Aires, CONICET, FONCYT, and the Fundación Antorchas. Juan Pablo Guerschman provided important help during manuscript preparation.

**REFERENCES**

Armesto JJ, Villagran C, Arroyo MK. 1995. Ecología de los bosques nativos de Chile. Santiago (Chile): Editorial Universitaria, Universidad de Chile. 470 p.

Box EO. 1981. Predicting physiognomic vegetation types with climate variables. *Vegetatio* 45:127-39.

Cabrera AL. 1976. Regiones fitogeográficas Argentinas. In: Parodi L, editor. *Enciclopedia Argentina de Agricultura y Jardinería*. Buenos Aires: Editorial Acme S.A.C.I. p. 1-85.

Cabrera AL, Wilkins A. 1973. *Biogeografía de América Latina*. Washington (DC): Editorial OEA. 120 p.

Chapin FS. 1993. Functional role of growth forms in ecosystem

- and global processes. In: Ehleringer JR, Field CB, editors. *Scaling physiological processes: leaf to globe*. London: Academic Press. p 287–312.
- De Fries RS, Hansen M, Townshend JRG, Sohlberg R. 1998. Global land cover classification at 8 km spatial resolution: the use of training data derived from Landsat imagery in decision tree classifiers. *Int J Remote Sens* 19:3141–68.
- Epstein HE, Lauenroth WK, Burke IC, Coffin DP. 1997. Regional productivity patterns of C<sub>3</sub> and C<sub>4</sub> functional types in the US Great Plains. *Ecology* 78:722–31.
- Fuentes E, Prenafeta S. 1988. *Ecología del paisaje en Chile central*. Santiago (Chile): Universidad Católica de Chile. 125 p.
- Goulden ML, Munger JW, Fan SM, Daube BC, Wofsy SC. 1996. Exchange of carbon dioxide by a deciduous forest: response to interannual climate variability. *Science* 271:1576–8.
- Guerschman J. 1998. *El uso de la tierra en regiones templadas de Argentina. Patrones, determinantes ambientales e impacto sobre el funcionamiento de los ecosistemas [thesis]*. Buenos Aires: Universidad de Buenos Aires. 80 p.
- Holdridge LR. 1947. Determination of world plant formations from simple climatic data. *Science* 105:367–8.
- Hord M. 1982. *Digital image processing of remotely sensed data*. New York: Academic Press.
- Hueck K. 1978. *Los bosques de Sudamérica*. Eschborn (Germany): GTZ. 476 p.
- [INDEC]. 1988. *Censo nacional agropecuario 1988: resultados generales*. Buenos Aires: Instituto Nacional de Estadísticas y Censos.
- [INTA-SAGYP]. 1990. *Atlas de suelos de la República Argentina, I-II*. Buenos Aires: INTA-SAGYP. 975 p.
- James ME, Kallury SNV. 1994. The pathfinder AVHRR land data set: an improved coarse resolution data set for terrestrial monitoring. *Int J Remote Sens* 15:3347–63.
- Jobbágy EG, Paruelo JM, León RJC. 1995. Estimación de la precipitación y de su variabilidad interanual a partir de información geográfica en el NW de Patagonia, Argentina. *Ecol Aust* 5:47–53.
- Jobbágy EG, Paruelo JM, León RJC. 1996. Vegetation heterogeneity and diversity in flat and mountain landscapes of Patagonia. *J Veg Sci*, 7:599–608.
- Jobbágy E, Sala O, Paruelo JM. Patterns and controls of primary production in the Patagonian steppe: a remote sensing approach. *Ecology*. Forthcoming.
- Leemans R, Cramer W. 1991. *The IIASA database for mean monthly values of temperature, precipitation and cloudiness on a global terrestrial grid. RR-91-18*. Luxembourg: International Institute of Applied Systems Analyses.
- León RJC, Bran D, Collantes M, Paruelo JM, Soriano A. 1998. Grandes unidades de vegetación de la Patagonia. *Ecol Aust*; 8:125–44.
- León RJC, Facelli JM. 1981. Descripción de una coenocline en el SO del Chubut. *Revista Facultad Agron* 2:163–71.
- Lloyd D. 1990. A phenological classification of terrestrial vegetation cover using shortwave vegetation index imagery. *Int J Remote Sens* 11:2269–79.
- Loveland TR, Belward AS. 1997. The IGBP-DIS global 1 km land cover data set. Discover: first results. *Int J Remote Sens* 18: 3289–95.
- Loveland TR, Merchant JW, Ohlen DO, Brown JF. 1991. Development of a land cover characteristics database for the conterminous US. *Photogram Eng Remote Sens* 57:1453–63.
- Loveland TR, Reed BC, Brown JF, Ohlen DO, Zhu Z, Yang L, Merchant JW. 2000. Development of a global land cover characteristics database and IGBP DIScover from 1 km AVHRR data. *Int J Remote Sens* 21:1303–30.
- Malanson GP, Westman WE, Yan YL. 1992. Realized versus fundamental niche functions in a model of chaparral response to climatic change. *Ecol Model* 64:261–77.
- Malingreau JP. 1986. Global vegetation dynamics, satellite observations over Asia. *Int J Remote Sens* 7:1121–46.
- Milchunas DG, Lauenroth WK. 1995. Inertia in plant community structure: state changes after cessation of nutrient enrichment stress. *Ecol Appl* 5:1995–2005.
- Morello J. 1958. *La provincia fitogeográfica del Monte*. *Opera Lilloana* 2:1–155.
- Mueller-Dombois D, Ellenberg H. 1974. *Aims and methods of vegetation ecology*. New York: Wiley. 547 p.
- Myneni RB, Keeling CD, Tucker CJ, Asrar G, Nemani RR. 1997. Increased plant growth in the northern high latitudes from 1981 to 1991. *Nature* 386:698–702.
- Nemani R, Running S. 1997. Land cover characterization using multitemporal red, near-IR, and thermal-IR data from NOAA/AVHRR. *Ecol Appl* 7:79–90.
- Paruelo JM, Aguiar MR, Golluscio RA, León RJC, Pujol G. 1993. Environmental controls of Normalized Difference Vegetation Index dynamics in Patagonia. *J Veget Sci* 4:425–8.
- Paruelo JM, Aguiar MR, León RJC, Golluscio RA, Batista WB. 1991. The use of satellite imagery in quantitative phytogeography: a case study of Patagonia (Argentina). *Quantitative approaches to phytogeography*. The Hague: Kluwer Academic Publishers. p. 183–204.
- Paruelo JM, Epstein HE, Lauenroth WK, Burke IC. 1997. ANPP estimates from NDVI for the central grassland region of the US. *Ecology* 78:953–8.
- Paruelo JM, Jobbágy EG, Sala OE, Lauenroth WK, Burke IC. 1998. Functional and structural convergence of temperate grassland and shrubland ecosystems. *Ecol Appl* 8:194–206.
- Paruelo JM, Lauenroth WK. 1998. Interannual variability of the NDVI curves and their climatic controls in North American shrublands and grasslands. *J Biogeog* 25:721–33.
- Paruelo JM, Lauenroth WK. 1995. Regional patterns of NDVI in North American shrublands and grasslands. *Ecology* 76:1888–98.
- Paruelo JM, Lauenroth WK, Epstein HE, Burke IC, Aguiar MR, Sala OE. 1995. Regional climatic similarities in the temperate zones of North and South America. *J Biogeog* 22:689–699.
- Pennington W. 1986. Lags in adjustment of vegetation to climate caused by the pace of soil development: evidence from Britain. *Vegetatio* 67:105–18.
- Prentice IC, Cramer W, Harrison SP, Leemans R, Monserud RA, Solomon AM. 1992. A global biome model based on plant physiology and dominance, soil properties and climate. *J Biogeog* 19:117–34.
- Prince SD. 1991. Satellite remote sensing of primary production: comparison of results for Sahelian grasslands 1981–1988. *Int J Remote Sens* 12:1301–11.
- Rao CRN, Chen J. 1995. Inter-satellite calibration linkages for the visible and near-infrared channels of the Advanced Very High Resolution Radiometer on the NOAA-7, -9 and -11 spacecraft. *Int J Remote Sens* 16:1931–42.
- Richards JF. 1993. *Land transformation*. In: Turner BL, Clark WC, Kater RW, Richards JF, Matthews JT, Meyer WB, editors. *The Earth as transformed by human action*. Cambridge, (UK): Cambridge University Press. p. 163–78.

- Sala OE, Parton WJ, Joyce LA, Lauenroth WK. 1988. Primary production of the central grassland region of the United States. *Ecology* 69:40–5.
- SAS. 1988. SAS/STAT user's guide. Release 6.03. Cary (NG): SAS Institute.
- Sellers PJ, Berry JA, Collatz GJ, Field CB, Hall FG. 1992. Canopy reflectance, photosynthesis, and transpiration. III. A reanalysis using improved leaf models and a new canopy integration scheme. *Remote Sens Environ* 42:187–216.
- Soriano A. 1956. Los distritos florísticos de la Provincia Patagónica. *Revista Invest Agropecuarias* 10:323–47.
- Soriano A. 1991. Rio de la Plata grasslands. In: Coupland RT, editor. *Natural grasslands: introduction and Western Hemisphere*. Amsterdam: Elsevier. p. 367–408.
- Soriano A, Paruelo JM. 1992. Biozones: vegetation units defined by functional characters identifiable with the aid of satellite sensor images. *Global Ecol Biogeog Lett* 2:82–9.
- Stephenson NL. 1990. Climatic control of vegetation distribution: the role of the water balance. *Am Nat* 135:649–70.
- Tou JT, Gonzalez RC. 1974. *Pattern recognition principles*. Reading (MA): Addison-Wesley.
- Tucker CJ, Townshend JR, Goff TE. 1985a. African land-cover classification using satellite data. *Science* 227:369–75.
- Tucker CJ, Vanpraet CV, Sharman MJ, Vanlittersum G. 1985b. Satellite remote sensing of total herbaceous biomass production in the Senegalese Sahel: 1980–1984. *Remote Sens Environ* 17:233–49.
- Valentini R, Baldocchi DD, Tenhunen JD. 1999. Ecological controls on land-surface atmospheric interactions. In: Tenhunen JD, Kabat P, editors. *Integrating hydrology, ecosystem dynamics, and biogeochemistry in complex landscapes*. Chichester (UK): Wiley. p. 117–46.
- Wessman C. 1992. Spatial scales and global change: bridging the gap from plots to GCM grid cells. *Ann Rev Ecol Syst* 23:175–200.
- Wessman C, Cramer W, Gurney RJ, Martin P, Mauser W, Nemani R, Paruelo JM, Peñuelas J, Prince SD, Running SW, and others. 1999. Remote sensing perspectives and insights for study of complex landscapes. In: Tenhunen JD, Kabat P, editors. *Integrating hydrology, ecosystem dynamics, and biogeochemistry in complex landscapes*. Chichester (UK): Wiley. p. 89–104.

## Appendix Description of the Ecosystem Functional Types

**01.De10.** This EFT is dominant in one of the main agricultural areas of temperate South America, the pampas. It is well represented in the southeastern portion of Buenos Aires province, located in the Argentine pampas. Soils are mainly Mollisols with high content of organic matter (INTA-SAGYP 1990). The potential vegetation of this area is grasslands codominated by C3 and C4 grasses (southern pampa grasslands) (Soriano 1991). Currently, the core of this EFT is devoted to wintercrops (INDEC 1988; Guerschman 1998). The dominance of wintercrops may be responsible for NDVI peaking in early spring (October). RREL shows intermediate values because of the presence of crops during winter months, which increases the minimum value of

NDVI. This EFT is also well represented in Chile in areas formerly dominated by temperate forests and now devoted to winter crops and pastures.

**02.Cd2.** This EFT occurs mainly in the most important summer crop area of Argentina, located in the northeastern part of Buenos Aires province (INDEC 1988; Guerschman 1998). Prior to colonization, grasslands dominated this region (rolling pampas) (Soriano 1991). Soils are well developed. Most of them are classified in the group of Argiudolls, with no limitations for agriculture (INTA-SAGYP 1990). The dominance of summer crops (soybeans and corn) may cause NDVI to peak in February (summer). The range of NDVI through the year is high. This EFT also occurs in the southern part of Chile's Central Valley, another important agricultural area of temperate South America.

**03.Ee10.** This EFT occurs in southwest Buenos Aires and eastern La Pampa in Argentina. There is less precipitation (600–700 mm) than in the two previous EFTs. The proportion of croplands decreases, while that of cultivated pastures increases. From a phytogeographical viewpoint, this EFT corresponds to a transition zone between the Río de La Plata grasslands and the *Prosopis sp* savannas of the Espinal. Wheat is the dominant crop (INDEC 1988; Guerschman 1998). Sown pastures are dominated by alfalfa and C3 grasses. Soils are, generally more coarse-textured than in the eastern part of the region. The most important taxonomic groups are Haplustolls and Hapludolls (INTA-SAGYP 1990). This EFT also occurs in the northern portion of the Chile's Central Valley, an area devoted to crops and pastures.

**04.Ce1.** This EFT is well represented in northwestern Buenos Aires, northeastern La Pampa, and southeastern Cordoba in Argentina; in northeast Uruguay and southern Brazil; and in the Andean foothills of Chile. It is the most extensive EFT of temperate South America. Potential vegetation corresponds to the inland pampa grasslands and southern campos (Soriano 1991) and the Mediterranean scrublands and woodlands. Soils are mainly Haplustolls and Hapludolls in the pampas and are more variable in the campos (INTA-SAGYP 1990). Sown pastures, sunflowers, soybeans, and corn are the main land uses (INDEC 1988; Guerschman 1998). The dominance of summer crops may delay the NDVI peak of NDVI, as compared to EFT 03. Probably due to the relatively high abundance of perennial pastures, 03 and 04 show a smaller variation of the NDVI through the year than EFTs 01 and 02.

**05.Bf12.** This EFT occupies the mesopotamic region in eastern Argentina and western Uruguay and has the highest NDVI-1 in temperate South Amer-

ica. It is dominated by pastures, native grasslands, and open savannas (Soriano 1991). Grazing maintains a short grass structure in most of the natural grasslands. Scattered trees of *Acacia sp.* and *Prosopis sp.* are frequent on the landscape. These rangelands receive more radiation than agricultural areas. Soils are fine-textured, and Vertisols are common (INTA-SAGYP 1990). The relatively mild winter and the dominance of perennial grasslands result in a low range of NDVI throughout the year.

**06.Ce11.** This EFT corresponds to the Flooding Pampa (Soriano 1991), a flat, poorly drained sub-region of the pampas. The dominant land cover is native perennial grass. Ungrazed grasslands may reach 40 cm in height, but the most common structure is short grass, with most of the biomass concentrated in the top 10 cm (Soriano 1991). Soils present hydromorphic and natric limitations to agriculture (INTA-SAGYP 1990; Guerschman 1998). NDVI shows peaks in spring and has a relatively low seasonality.

**07.Bd11.** This EFT occurs in an area originally dominated by deciduous forest of *Nothofagus obliqua* and *Nothofagus procera* (Hueck 1978). Forests are still the dominant land cover, although part of the native deciduous forest has been replaced by *Pinus sp.* plantations. Precipitation increases from north to south and across topographic gradients. Temperatures are mild due to the influence of the Pacific Ocean and are also influenced by topography (Armesto and others 1995). Soils are mainly volcanic. Sixty-two percent of southern Chile is occupied by Andepts. This EFT is very productive (high NDVI-1) and exhibits a high seasonality.

**08. Ea1.** This EFT, which occurs in the most productive forests of the temperate areas of South America, is almost completely restricted to Chile. Precipitation often amounts to more than 2000 mm, and the topography creates important differences

in vegetation. *Fitzroya cupressoides*, *Nothofagus dombeyii*, and *Nothofagus pumilio* are the most important tree species of these forests. The NDVI pattern of this EFT is highly influenced by cloud cover, which may lead to an underestimation of the NDVI-1. A high proportion of the images used in this study had reduced NDVI values due to cloud contamination. Ea1 is also represented in the pampas in an area dominated by summer crops.

**09.Jc1.** This EFT is found in southern Chile and Argentina. It occupies an area dominated by deciduous forests of *Nothofagus* (*N. pumilio* and *N. betuloides*) and the magellanic tundra. As in the case of the evergreen forests, cloud contamination makes it

difficult to interpret the functional characteristics of the EFT.

**10.Fe1.** This EFT occupies an area formerly dominated by xerophytic woodlands (open forests) and savannas (Cabrera 1976) in northern La Pampa, eastern San Luis, and western Cordoba. It includes the southern portion of the Sierras Pampeanas (Cordoba and San Luis). Agriculture (mainly summer crops) is marginal due to the low mean annual precipitation (500–700 mm). Most precipitation occurs during the summer. Perennial pastures of *Eragrostis curvula* are common in this area. Entisols are the dominant soils.

**11.Gf12.** This EFT corresponds to a broad ecotone between the evergreen shrub steppes and the agriculture-dominated EFTs of the pampas and the Espinal. The transition is driven by a gradual change in mean annual precipitation from 300 to 500 mm. Croplands and grasslands disappear in areas with less than 550 mm of MAP and are replaced by a group of tall evergreen shrubs of the genus *Larrea* or isolated small tree individuals of *Geoffrea decorticans*. C3 grasses dominate the understory. The main functional change across this transition is the decrease in NDVI-1 associated with the reduction in MAP. Aridisols (orthids) and Entisols (psamments) are the most conspicuous soil units (INTA-SAGYP 1990).

**12.Ih3.** This EFT is dominant in San Juan and northern Mendoza (Argentina) and corresponds to an area dominated by evergreen shrubs of the genus *Larrea* (Monte phytogeographical province) (Cabrera 1976). Soils are mainly Entisols (psamments). NDVI peaks late in the growing season (March), and the relative range of NDVI is very low due to the dominance of evergreen shrubs.

**13.Jh10.** This EFT occupies a northwest–southeast band adjacent to the previous EFT. On average, precipitation is more evenly distributed through the year than in Ih3. Evergreen shrubs of the genus *Larrea* are still dominant. From a functional viewpoint, the main difference from the other evergreen shrub steppe is the timing of the NDVI peak, which occurs in spring (October).

**14.Ig11.** This EFT is well represented in the densely populated central part of Chile. It also occurs as small islands along the Monte–Patagonia border in Argentina. Potential vegetation includes scrublands and sclerophyllus woodlands (Hueck 1978; Fuentes and Prenafeta 1988). Most of the area has been heavily modified by humans. NDVI peaks early (September–October) due to the winter distribution of precipitation.

**15.Gb11.** This EFT occurs along a steep gradient of precipitation on the eastern side of the Andes

(Jobbágy and others 1995). The western border corresponds to the ecotone between grasslands and forests. At the eastern border, there is a gradual transition to the grass–shrub steppes of Patagonia (León and Facelli 1981). The complex topography of the area has a variable effect on water availability and creates a mosaic of plant communities (Jobbágy and others 1996). *Festuca pallelescens* is the dominant grass, but total cover is less than 60%. Soils are mainly Mollisols (Haploborolls and Haploxerolls) (INTA-SAGYP 1990). This EFT shows the highest NDVI-1 among the Patagonian units. NDVI is very seasonal and peaks later than in the other Patagonian EFTs. The timing of the NDVI peak is positively related to water availability (E. G. Jobbágy and others forthcoming). This EFT is also observed in irrigated areas covered by perennial crops, such as the Río Negro Valley, which is located within a matrix of Jh10.

**16.Ie11.** This EFT occurs along a gradual transition between the western grass steppes and the semideserts and shrub steppes of Patagonia. Aridisols are the dominant soils (INTA-SAGYP 1990). The cover of grasses is still important in this EFT. As in most of the extra-Andean Patagonia, the NDVI peak occurs in November. It is well represented in southern Santa Cruz between the *Festuca gracilima* grasslands and the *Nassauvia sp.* semideserts. *Verbena*

*tridens* is an important component of this community (León and others 1998).

**17.Jg11.** There is no clear geographical limit between this EFT and Ie11 and If12. The relative cover of grasses and shrubs changes gradually as mean annual precipitation decreases. It is well represented in northern Patagonia and in the Argentine provinces of Chubut, Río Negro, and Santa Cruz. It is one of the largest EFTs of temperate South America.

**18.Kg10.** This EFT is the least productive of temperate South America. Its distribution is restricted to the Santa Cruz and Chubut provinces in Argentina. The EFT corresponds with semideserts of *Nassauvia glomerulosa* and *Nassauvia ulicina* (Paruelo and others 1991). As in the previous EFTs, Aridisols are the most important soils (INTA-SAGYP 1990). Among the Patagonian EFTs, the semideserts showed the earliest NDVI peak (October) due to low water availability (E. G. Jobbágy and others forthcoming).

**19.Jf12.** This EFT has a disjunctive distribution. It is well represented in the highest part of the central Andes and the southwestern part of Patagonia, in the transition between the grass steppe and the shrub steppe. In southern Patagonia, it is mainly associated with high plateaus. The delayed NDVI peak in this case may be related to the late start of the growing season due to low winter temperatures.